

Proceeding Paper

Searching for Muon to Electron Conversion with the COMET Experiment †

Sam Dekkers  on behalf of the COMET Collaboration

School of Physics and Astronomy, Monash University, Clayton, VIC 3800, Australia; sam.dekkers1@monash.edu
† Presented at the 23rd International Workshop on Neutrinos from Accelerators, Salt Lake City, UT, USA, 30–31 July 2022.

Abstract: Charged lepton flavour violation processes provide a well-motivated experimental probe into new physics beyond the Standard Model. Muon to electron conversion is one example that the COMET experiment aims to measure with increased sensitivity over previous searches. Taking a staged approach, the COMET experiment will measure muon to electron conversion with sensitivities of $\mathcal{O}(10^{-15})$ and $\mathcal{O}(10^{-17})$ in Phase-I and Phase-II, respectively. An important initial low-intensity beam run, Phase- α , is also planned to begin in 2023 with Phase-I following in 2024. This article summarises the COMET experiment and the recent progress made towards the beginning of physics runs.

Keywords: muon physics; detectors; flavour physics; J-PARC; particle physics experiment

1. Introduction

Charged lepton flavour violation (CLFV) provides a unique experimental probe in searches for physics beyond the Standard Model. It is known and understood that flavour violation can be observed in the quark and neutral lepton sectors of the Standard Model, leaving the question open as to whether it exists in the charged lepton sector. Muon to electron (μ - e) conversion is one example of CLFV, in which a muon captured by an atomic nucleus is converted coherently in an electron. If one only considers Standard Model physics plus neutrino oscillations, μ - e conversion is extremely suppressed to the point of being unobservable, with conversion ratios in the range of $\mathcal{O}(10^{-55})$. Many beyond Standard Models (BSM), however, predict it to be enhanced with conversion ratios of up to $\mathcal{O}(10^{-15})$, which is within the modern experimental sensitivity reach, making μ - e conversion a powerful probe, as any observation would be unambiguous evidence of new physics. Many well-motivated BSMs facilitate CLFV, such as models that introduce supersymmetric light particles, leptoquark models, and heavy Z' models (e.g., [1,2] and summarised in [3]). One can also consider effective field theories that introduce dipole operators and four-fermi contact operators which, when combined with bounds from related CLFV experiments, such as $\mu \rightarrow e\gamma$ and $\mu \rightarrow eee$, can reveal information about the structure of the new physics [4].

To observe μ - e conversion experimentally, muons are stopped in some target materials where they transition to the 1s state of a nucleus, after which they decay with some target-material-dependent lifetime. Muons undergoing μ - e conversion will have the distinct signature of a single monoenergetic electron with a momentum of $E_e \approx 104.97$ MeV [5], accounting for energy losses due to nuclear recoil and the muon binding with the nucleus. The major background of any measurement of μ - e conversion will come from the Standard Model muon decay, referred to as decay in orbit (DIO) for captured muons. While most DIO-produced electrons will be of low momentum and simple to suppress, the DIO momentum spectrum does reach the μ - e conversion momentum range when considering the sensitivity levels of next-generation μ - e conversion experiments [6]. This means an excellent momentum resolution is required in addition to other types of background suppression, such



Citation: Dekkers, S., on behalf of the COMET Collaboration. Searching for Muon to Electron Conversion with the COMET Experiment. *Phys. Sci. Forum* **2023**, *8*, 4. <https://doi.org/10.3390/psf2023008004>

Academic Editor: Yue Zhao

Published: 27 June 2023



Copyright: © 2023 by the author. Licensee MDPI, Basel, Switzerland. This article is an open access article distributed under the terms and conditions of the Creative Commons Attribution (CC BY) license (<https://creativecommons.org/licenses/by/4.0/>).

as beam-related backgrounds and cosmic muons. The Coherent Muon to Electron Transition (COMET) experiment [3] is one such next-generation experiment that searches for μ - e conversion with the greatest sensitivity yet surpasses the conversion ratio limit of 7.0×10^{-13} for μ - e conversion in gold set by SINDRUM II [7].

2. The COMET Experiment

2.1. Overview

To search for the μ - e conversion in aluminium, the COMET experiment is being constructed in Hadron Hall at the Japan Proton Accelerator Research Complex (J-PARC) in Tokai, Ibaraki, Japan. The COMET experiment will adopt a phased structure, including a pre-physics run beam line commissioning Phase- α and two physics runs, Phase-I and Phase-II, and is expected to reach sensitivity limits of 3.1×10^{-15} [3] and 1.4×10^{-17} [8], respectively. In order to improve on previous sensitivity limits, COMET requires high statistics and excellent background suppression as well as excellent momentum resolution to separate the signal from the tail end of the DIO electron spectrum. A pulsed beam structure will be used in order to remove beam-related backgrounds, while optimised curved solenoids and dipole fields will be used to remove high-momentum backgrounds during muon beam transport. Detectors are optimised in both Phase-I and -II to suppress low-momentum electron events, and veto detectors are used in both phases to remove cosmic muon events. An overview of the three phases is shown in Figure 1 and can be summarised as follows:

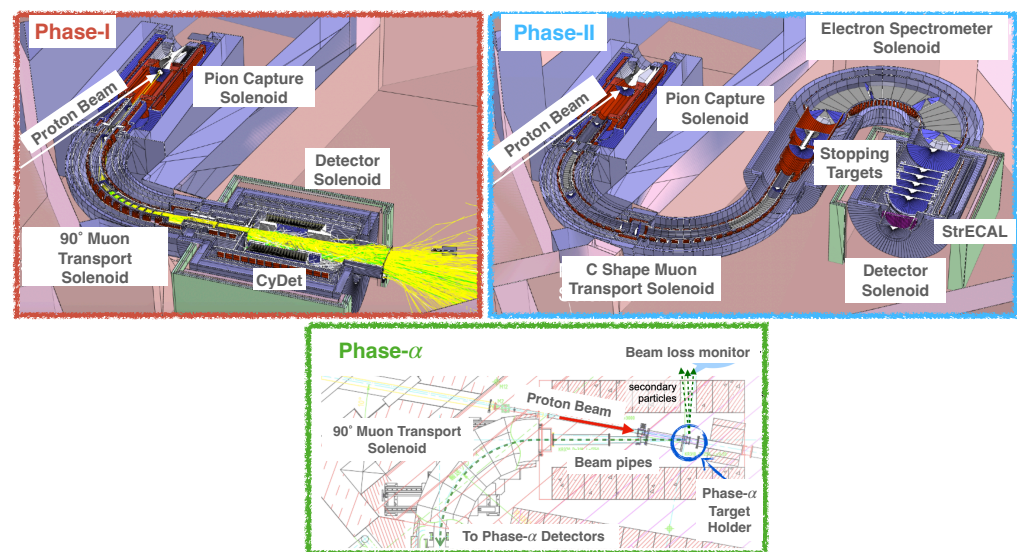


Figure 1. The COMET experiment is taking a phased approach with Phase-I (top left) and Phase-II (top right). An initial low-intensity beam run, Phase- α (bottom centre), will take place first.

Phase- α : Phase- α is a low-intensity beam commissioning run that is essential for Phase-I preparations. Phase- α will include a number of important studies, including further proton beam extinction measurements, studies on the properties of the COMET muon beam, and transport solenoid selection capabilities, pion yield and cross-sectional measurements, secondary beam particle measurements, and further validation studies of COMET simulations.

Phase-I: A pulsed proton beam will be used to generate the world's highest intensity muon beam producing an order of $\mathcal{O}(10^{18})$ muons that will be stopped on aluminium targets, resulting in approximately 1.2×10^9 muons stopped per second. Charge and momentum selection of muons is provided by a curved solenoid with optimised dipole fields. The main physics detector surrounding the stopping targets is called the Cylindrical Detector (CyDet) system, and this is further discussed in Section 2.3. Phase-I is expected to

involve the collection of physics data for 150 days beginning in 2024. The full details are outlined in [3].

Phase-II: In Phase-II, the collection of physics data for 260 days following Phase-I with increased proton beam power is planned. This will improve sensitivity limits over Phase-I with some key design factors being the usage of a full C-shaped muon transport solenoid for further beam suppression, an additional curved electron spectrometer for further suppression of DIO electrons and beam-related backgrounds, and the use of an upgraded straw tracker + electron calorimeter (StrECAL) detector for physics measurements.

2.2. Proton Beam, Pion Capture, and Muon Transport

The 30 GeV main ring at J-PARC provides the 8 GeV proton beam used for the COMET experiment with a pulsed structure in order to avoid the majority of the beam-related backgrounds and using approximately 1 μs spaced bunches to match the lifetime of muonic aluminium. In Phase-I, the beam power will be 3.2 kW, which will increase to 56 kW for Phase-II. Recent beam commissioning measurements showed interbunch extinction protons to be $\mathcal{O}(10^{-10})$, meeting the requirements for Phase-I [9]. The proton beam will be impinging on a graphite pion production target in Phase-I and upgraded to tungsten in Phase-II for increased pion yields. A 5 T capture solenoid will be used to direct pions into the muon transport solenoid. In Phase-I, a 90° curved transport solenoid will be used, and this will be upgraded to a full C-shaped solenoid for Phase-II. The muons produced from pion decay inside the transport solenoid follow a helical trajectory where an additional tuned dipole field is used to compensate for drift and allow for momentum selection in conjunction with beam collimators at the end. Low-momentum muons are selected for and directed into the stopping targets.

2.3. Muon Stopping Targets and Detectors

The stopping target system for Phase-I consists of 17 aluminium discs, 100 mm in radius and 200 μm in thickness, present in the centre of the detector region. Aluminium was chosen for COMET as it provides a good tradeoff between the muon capture rate, DIO electron endpoint tail, and muonic atom lifetime which, for muonic aluminium, is 864 ns [10]. A support structure for the stopping targets will be integrated into the Phase-I detector system's support structure.

As mentioned in Section 2.1, the CyDet system provides the main physics measurements for Phase-I. At a high level, a Cylindrical Drift Chamber (CDC) provides the tracking and momentum information for the stopped muon decay products, and a Cylindrical Trigger Hodoscope (CTH) provides additional timing information, triggering on high-momentum particles. The CyDet system is surrounded by a 1 T magnetic detector solenoid such that charged particle products follow a helical trajectory towards the ends of the detector region. High radiation levels will be present in the detector region with 10^{12} $n_{\text{eq}}/\text{cm}^2$ neutrons and 1 kGy gamma rays expected [11].

The CDC detector is a drift chamber consisting of 20 concentric wire layers (including two guard layers) with alternating positive and negative stereo angles of ± 70 mrad. A total of 4986 25 μm gold-plated tungsten sense wires and 14,562 126 μm pure aluminium field wires are used in a $\text{He:iC}_4\text{H}_{10}$ gas mixture. A large inner wall radius of 496 mm was designed such that low-momentum DIO electrons will be suppressed from reaching the sense layers within the detector's solenoid field. The CDC was also designed such that high-momentum signal electrons will be contained within the detection volume for better momentum resolution. Overall, a momentum resolution of better than 200 keV/c is expected for signal electrons. The CDC uses Belle-II-based RECBE boards for readout [12].

The CTH detector consists of two layers of 64 concentric scintillator counter rings located on both the upstream and downstream sides of the CDC detector, with the photon readout provided by multipixel photon counter (MPPC) photodetectors via plastic optical fibre bundles due to the high radiation levels. The main principle behind its background suppression is the four-fold coincidence in the counter layers, as low momentum back-

grounds will not penetrate this far. The support structure includes an inner lead shielding layer as well as providing a tilt angle to the counters that is optimised for signal electron acceptance. The CTH detector requires a timing resolution of better than 1 ns.

A cosmic ray veto (CRV) detector is critical for excluding atmospheric muon events in both Phase-I and Phase-II. The CRV detector provides both passive shielding through its inner-wall materials and active shielding through four layers of scintillator modules read out by silicon photomultipliers. In Phase-I, this detector will cover the CyDet region and bridge solenoid at the end of the muon transport solenoid and has a requirement of 99.99% efficiency and a dead time of less than 5%.

The StrECAL detector will be the main physics detector for Phase-II, with an initial version being tested in Phase-I. The straw tube tracker, consisting of five straw stations with four straw planes each, will provide momentum information, while the electron calorimeter will provide energy, timing, and positional information. In Phase-I, the straws will be 20 μm mylar + 70 nm aluminium thick with a 9.8 mm ϕ gauge, while in Phase-II, the straws will be reduced to 12 μm mylar + 70 nm aluminium thick with a 5.0 mm ϕ gauge. A gas mixture of Ar:Ethane (50:50) is used and the average spatial resolution measured is less than 150 μm which allows for better than 200 keV/c momentum resolution [13]. In terms of the electron calorimeter, LYSO crystals are being used with avalanche photodiodes for readout. In a 105 MeV electron prototype test, it was shown that the energy resolution (σ_E/E) is 4%, the positional resolution (σ_x) is 0.6 cm, and the time resolution (σ_t) is 0.5 ns, which all meet the necessary requirements [13]. The Phase-II design will improve the LYSO crystal coverage.

2.4. Software, Trigger and DAQ System

The COMET collaboration utilises an offline software framework based on the ND280 detector software framework from the T2K experiment that allows for full physics simulations with realistic geometry and magnetic field implementation as well as full detector calibration, reconstruction, and analysis. Mass production runs of simulation data have been used to optimise the COMET experiment's design and improve offline event reconstruction and tracking.

The trigger system for COMET is essential for suppressing the number of background events. The Phase-I trigger system collects information from the CDC and CTH detectors via front-end and merger boards that feed into an FC7 [14] central trigger board that makes the final decision. The current classification system is based on a GBDT filter that allows for high-level suppression of CDC hits which, when combined with the CTH trigger information, suppress the overall trigger rate to 13 kHz with only 3.2 μs latency [15]. COMET will also use a MIDAS-based DAQ system [16] that provides a total throughput of 1 GB/s.

3. COMET Status

All aspects of COMET are continuously progressing on schedule for Phase- α in 2023 and Phase-I in 2024. At J-PARC, the C-Line of the proton beamline has been completed up to the Hadron Hall where COMET is located. This puts the beamline on track for completion in 2022, ready for Phase- α . The muon transport solenoid, which is already located on site, has had its first cooling and excitation tests recently completed, and preparations for the pion capture solenoid assembly are ongoing. In terms of Phase- α , which will not require the pion capture solenoid to be completed, beam tests for its detectors were also recently performed and analysis is ongoing.

The CDC detector, which has been completed since 2016 with readout and testing performed since 2019 [17], was recently moved on site to J-PARC where testing continues in addition to cooling tests on the front end electronics also recently performed. Steady progress has been made on the CRV detector too with the first scintillator module constructed, and full construction is anticipated in 2023. Production of a muon stopping target holder prototype is also underway. The Phase-I version of the StrECAL detector system is

also on schedule for completed construction in 2023 with the first straw station out of five completed and the second station well in progress. The ECAL support structure has also been completed with crystal installation and detector construction in progress, and readout electronics production has begun.

In terms of COMET's software updates, the sixth mass production run of simulation data is in progress, which will include the most up-to-date configuration of COMET as we approach Phase-I. Further efforts have also been made to improve the trigger system for Phase-I. The current GBDT-based system has already been shown to meet the trigger rate and latency requirements for Phase-I, but further improvements are currently being explored based on the real-time machine learning techniques discussed in [18]. Trigger schemes for other exotic physics measurements, such as muon to positron conversion, are also being explored. Physics motivations for such measurements can be found in [19].

A significant update has also been made to the design of the CTH detector, which has been updated from the previous design discussed in [3]. All counters are now scintillators with the number of scintillator counters per ring increased from 48 to 64 segments. These counters will now be read out by MPPC instead of with photomultiplier tubes, allowing for a reduced cost system with easier replacement during Phase-I data collection. Recent progress on the development of the CTH detector has been made, including photon yield measurements [20], MPPC irradiation plus cooling system tests and preliminary prototype counter beam measurements using 100 MeV electrons at the Australian Synchrotron, as shown in Figure 2. A prototype section of the support structure has also been produced. Future beam tests will be critical for evaluating the positional and angular photon yield dependence of the counters as well as for evaluating the timing resolution. A prototype preamplifier readout system has also been developed to feed timing and energy deposition information from each counter to the trigger system. The CTH detector is expected to be constructed in 2023, ready for Phase-I.

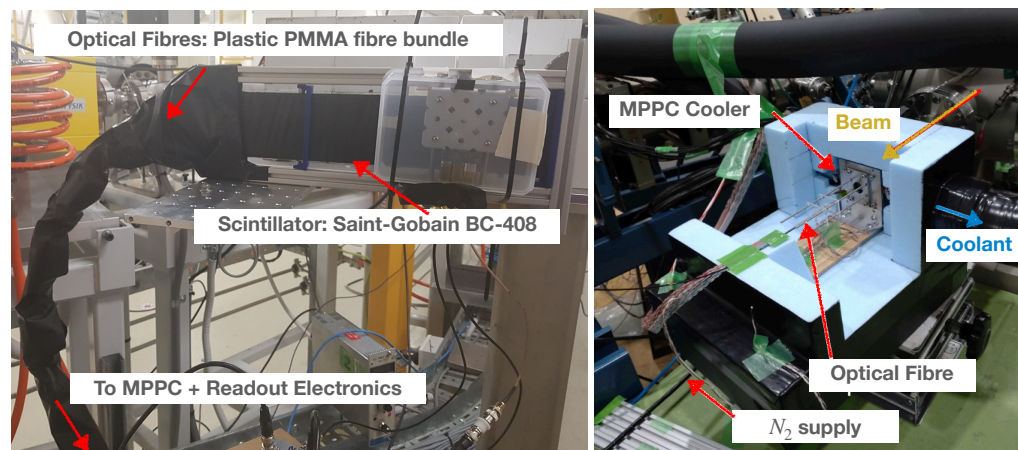


Figure 2. The CTH detector provides timing information for COMET Phase-I and utilises scintillator counters with MPPC photodetectors for photon readout. Recent progress includes preliminary beam tests with prototype counters using 100 MeV electrons at the Australian Synchrotron (**left**) and MPPC irradiation and cooling tests (**right**).

4. Conclusions

The COMET experiment will search for μ - e conversion in muonic aluminium, reaching the highest experimental sensitivity yet utilising a phased approach. The low-intensity beam run, Phase- α , which is an important milestone for COMET to reach its physics goals is on track to begin in 2023. Phase-I, which expects to reach a single-event sensitivity of 3.1×10^{-15} , is also on schedule to begin its physics data collection run in 2024, while Phase-II will begin shortly after, while increasing the single-event sensitivity to 1.4×10^{-17} , and R&D efforts are happening concurrently with the construction of Phase-I systems. This

proceeding article provides an overview of the COMET experiment and the collaboration's most recent progress in working towards the physics goals set for each phase.

Funding: The author was supported for this conference in part by Australian Research Council's Discovery Projects funding scheme (project DP200101562) and in part by Monash University.

Institutional Review Board Statement: Not applicable.

Informed Consent Statement: Not applicable.

Data Availability Statement: Data sharing not applicable No new data were created or analyzed in this study. Data sharing is not applicable to this article.

Acknowledgments: This was written on behalf of, and the author acknowledges strong support from, the COMET collaboration. We acknowledge support from JSPS, Japan; ARC, Australia; Belarus; NSFC, China; IHEP, China; IN2P3-CNRS, France; CC-IN2P3, France; SRNSF, Georgia; DFG, Germany; JINR; IBS, Korea; RFBR, Russia; STFC, United Kingdom; and the Royal Society, United Kingdom. The views expressed herein are those of the author and are not necessarily those of the Australian Government or Australian Research Council.

Conflicts of Interest: The author declares no conflict of interest.

References

1. Kuno, Y.; Okada, Y. Muon decay and physics beyond the standard model. *Rev. Mod. Phys.* **2001**, *73*, 151. [[CrossRef](#)]
2. Dorner, I.; Fajfer, S.; Greljo, A.; Kamenik, J.F.; Konik, N. Physics of leptoquarks in precision experiments and at particle colliders. *Phys. Rept.* **2016**, *641*, 1–68. [[CrossRef](#)]
3. The COMET Collaboration. COMET Phase-I technical design report. *Prog. Theor. Exp. Phys.* **2020**, *2020*, 033C01. [[CrossRef](#)]
4. Cirigliano, V.; Kitano, R.; Okada, Y.; Tuzon, P. Model discriminating power of $\mu \rightarrow e$ conversion in nuclei. *Phys. Rev.* **2009**, *D80*, 013002.
5. Heeck, J.; Szafron, R.; Uesaka, Y. Isotope dependence of muon decay in orbit. *Phys. Rev. D* **2022**, *105*, 053006. [[CrossRef](#)]
6. Czarnecki, A.; Garcia i Tormo, X.; Marciano, W.J. Muon decay in orbit: Spectrum of high-energy electrons. *Phys. Rev. D* **2011**, *84*, 013006. [[CrossRef](#)]
7. Bertl, W.; Engfer, R.; Hermes, E.A.; Kurz, G.; Kozlowski, T.; Kuth, J.; Otter, G.; Rosenbaum, F.; Ryskulov, N.M.; van der Schaaf, A.; et al. A search for μ - e conversion in muonic gold. *Eur. Phys. J. C* **2006**, *47*, 337. [[CrossRef](#)]
8. Oishi, K. Study of Sensitivity to Search for a Charged Lepton Flavor Violating Process. Ph.D. Thesis, Kyushu University, Kyushu, Japan, 2021.
9. Nishiguchi, H.; Fukao, Y.; Igarashi, Y.; Mihara, S.; Moritsu, M.; Ueno, K.; Hashimoto, Y.; Muto, R.; Tomizawa, M.; Tamura, F.; et al. Extinction Measurement of J-PARC MR with 8 GeV Proton Beam for the New Muon-to-Electron Conversion Search Experiment—COMET. In Proceedings of the 10th International Particle Accelerator Conference (IPAC2019), Melbourne, Australia, 19–24 May 2019; pp. 4372–4375.
10. Suzuki, T.; Measday, D.F.; Roalsvig, J.P. Total nuclear capture rates for negative muons. *Phys. Rev. C* **1987**, *35*, 2212. [[CrossRef](#)] [[PubMed](#)]
11. Nakazawa, Y.; Fujii, Y.; Gillies, E.; Hamada, E.; Igarashi, Y.; Lee, M.; Moritsu, M.; Matsuda, Y.; Miyazaki, Y.; Nakai, Y.; et al. Radiation hardness study for the COMET Phase-I electronics. *Nucl. Instrum. Methods Phys. Res. A Accel. Spectrom. Detect. Assoc. Equip* **2020**, *955*, 163247. [[CrossRef](#)]
12. Uchida, T.; Ikeno, M.; Iwasaki, Y.; Saito, M.; Shimazaki, S.; Tanaka, M.; Taniguchi, N.; Uno, S. Readout electronics for the central drift chamber of the Belle II detector. In Proceedings of the 2011 IEEE Nuclear Science Symposium Conference Record, Valencia, Spain, 23–29 October 2011; pp. 694–698.
13. Nishiguchi, H. StrECAL system for COMET Phase-I and Phase-II. Presented at the 22nd International Workshop on Neutrinos from Accelerators (NuFact 2021), Cagliari, Italy, 6–11 September 2021.
14. Pesaresi, M.; Marin, M.B.; Hall, G.; Hansen, M.; Iles, G.; Rose, A.; Vasey, F.; Vichoudis, P. The FC7 AMC for generic DAQ & control applications in CMS. *J. Instrum.* **2015**, *10*, C03036.
15. Nakazawa, Y.; Fujii, Y.; Ikeno, M.; Kuno, Y.; Lee, M.; Mihara, S.; Shoji, M.; Uchida, T.; Ueno, K.; Yoshida, H. An FPGA-based trigger system with online track recognition in COMET Phase-I. *IEEE Trans. Nucl. Sci.* **2021**, *68*, 8. [[CrossRef](#)]
16. Ritt, S.; Amaudruz, P.A. New components of the MIDAS data acquisition system. In Proceedings of the 11th IEEE NPSS Real Time Conference Record, Sante Fe, NM, USA, 14–18 June 1999; pp. 116–118.
17. Wu, C.; Wong, T.S.; Kuno, Y.; Moritsu, M.; Nakazawa, Y.; Sato, A.; Sakamoto, H.; Tran, N.H.; Wong, M.L.; Yoshida, H.; et al. Test of a small prototype of the COMET cylindrical drift chamber. *Nucl. Instrum. Methods Phys. Res. Sect. A* **2021**, *1015*, 165756. [[CrossRef](#)]

18. Fujii, Y. Online machine learning based event selection for COMET Phase-I. Presented at the 23rd International Workshop on Neutrinos from Accelerators (NuFact 2022), Salt Lake City, UT, USA, 31 July–6 August 2022.
19. Lee, M.; MacKenzie, M. Muon to Positron Conversion. *Universe* **2022**, *8*, 227. [[CrossRef](#)]
20. Fujii, Y.; Aoki, M.; Dekkers, S.; Nash, J.; Tojo, J.; Ueno, K.; Wakabayashi, H. Studies of optical fibre and SiPM readout system for the Cylindrical Trigger Hodoscope in COMET Phase-I. Presented at the Lepton Photon 2021, Zenodo, Manchester, UK, 9–14 August 2021.

Disclaimer/Publisher's Note: The statements, opinions and data contained in all publications are solely those of the individual author(s) and contributor(s) and not of MDPI and/or the editor(s). MDPI and/or the editor(s) disclaim responsibility for any injury to people or property resulting from any ideas, methods, instructions or products referred to in the content.